Identification of Free-Field Soil Properties Using NUPEC Recorded Ground Motions

J. Xu[1], C. Costantino[1], C. Hofmayer [1], A. Murphy [2], N. Chokshi [2], Y. Kitada [3],

1) Brookhaven National Laboratory, Upton, New York 11973-5000, USA
2) U.S. Nuclear Regulatory Commission, Washington, D.C. 20555-0001, USA
3) Nuclear Power Engineering Corporation, Tokyo, Japan

ABSTRACT

Over the past twenty years, the Nuclear Power Engineering Corporation (NUPEC) of Japan has conducted a series of field model test programs to investigate various aspects of soil-structure interaction (SSI) effects on nuclear power plant structures, including embedment and dynamic structure-soil-structure interaction (SSSI) effects. As part of a collaborative agreement between the US Nuclear Regulatory Commission (NRC) and NUPEC, Brookhaven National Laboratory (BNL) performed a numerical analysis to predict the free field soil profile using industry standard methods and the recorded free field responses to actual earthquake events. This paper describes the BNL free-field analyses, including the methods and the analysis results and their comparison to recorded data in the free field. The free-field soil profiles determined from the BNL analyses are being used for both the embedment and SSSI studies, the results of which will be made available upon their completion.

INTRODUCTION

As part of the Seismic Proving Test program for nuclear power plant (NPP) structures, the Nuclear Power Engineering Corporation (NUPEC) of Japan has conducted a series of field model test programs to ensure the adequacy of methodologies employed for seismic analyses of NPP structures [1,2]. Large-scale realistic model structures for reactor and turbine buildings were constructed at a site, which experiences frequent small to median earthquakes with maximum free field ground shaking up to 174 gal. The NUPEC test program has collected a large amount of recorded data from these model structures and the free field, which can be used to investigate various aspects of soil-structure interaction (SSI) effects, including embedment and dynamic structure-soil-structure interaction (SSSI) effects. As part of collaborative efforts between the United States and Japan on seismic issues, the US Nuclear Regulatory Commission (NRC) and Brookhaven National Laboratory (BNL) are participating in this program to apply the industry practice to predict both the free field and structural responses to recorded earthquake events, including the SSSI effect, and to interpret the observed data. This paper provides a description of the BNL free field analysis.

NUPEC provided recorded data from five earthquakes to BNL, including down-hole accelerometer measurements in the free field and structural responses. The BNL free field analysis applied the Fourier ratio method with non-linear least square fitting technique to correlate the recorded free-field earthquake motions, therefore back-calculating the soil properties. Similar applications can be found in Lotung and Port Island experiments [3,4]. The strain dependent modulus degradation relationships for the NUPEC site were determined by correlating the down-hole recordings to several published laboratory tests [5,6,7,8], in conjunction with a 1-D convolution model for vertically propagated shear waves. In order to identify the propagation mechanism of seismic waves associated with the recorded earthquakes, the Arias energy intensity [9,10] was calculated for the recorded earthquakes as they traveled across the site.

This paper contains four sections. Section 2 describes the method used for the BNL free field analysis. Discussions on the analysis results are provided in Section 3, including the back calculated soil properties that produce the soil column transfer functions, which retrofit soil amplifications computed from recorded free field earthquake motions along a down-hole array. Section 3 also discusses the selection of the modulus degradation relationships by correlating the down-hole recordings to the published laboratory data. Finally, conclusions are drawn in Section 4.

ANALYSIS TECHNIQUES

In the context of the 1D site model to be used for the BNL free field analysis, the wave propagating mechanisms associated with the recorded free-field motions need to be appropriately identified in order to screen out those records with wave types that are inconsistent with the 1D site model. The remaining records are analyzed using the Fourier ratios with the Levenburg-Marquadt non-linear least square fitting algorithm. In the following subsections, the technique used to analyze recorded free-field motions is first described, followed by a description of the Fourier ratio method.

Arias Intensity for Energy Transmission of Seismic Waves through Soils

At the NUPEC test site, a series of seismometers were placed at different depths along two down-hole arrays in the free field (referred to as the old and new free-field points) to record earthquake events that traveled through the site. An accurate measurement of the energy content of these seismometers on a time scale would enable examination of the wave propagation

of the seismic motion in the free field. This can be accomplished using the Arias intensity, which is represented by the following function

$$I_g(t) = \frac{\pi}{2g} \int_0^t \ddot{x}_g^{\,2}(\tau)\, d\tau \qquad (1)$$

where $\ddot{x}_g(\tau)$ represents an accelerogram recorded at a down-hole station and g is the gravitational acceleration.

To confirm an upward propagating motion, the Arias intensity computed for the down-hole seismometers located between rock and ground surface in the free field should show an initial built-up of energy in the rock seismometer with energy increasing as it propagates upward. Eventually the domination of energy should be established in the surface seismometer. On the other hand, for seismic motions with strong surface wave characteristics, which are usually associated with epicenter distances of more than 100m, the Arias intensity plots for the down-hole seismometers would not show a clear upward energy movement. BNL applied this technique to the recorded earthquake motions at both the old and new free-field points for selecting the motions that are consistent with the 1D site model.

Fourier Ratios with the Levenburg-Marquadt Non-Linear Least Square Fitting Algorithm

The Fourier ratio technique has been used extensively in studies for Treasure Island and Taiwan (Lotung and Hualein) sites to back-calculate the in-situ soil properties [3]. It was also employed by investigators in Japan [4] to identify the site soil properties at Port Island, Japan. The technique involves matching the theoretical transfer function to the actual amplifications in terms of Fourier spectral ratios computed from down-hole accelerometer recordings, and back-calculating the soil properties by iterations. It should noted that the procedure is used for determining the low strain soil properties in this study, although it could also be applied to identify strain-dependent properties, in which case both the shear wave velocity and hysteretic damping values associated with the soil column should be considered. A brief description of the Fourier ratio technique and its computer implementation for use in the free field analysis is provided below.

Assuming that the laboratory tests are used as the best estimates of the soil column, the identification process of the actual dynamic characteristics of the soil deposits can be formulated as a conditional non-linear least square minimization problem, which is stated as

$$\underset{v_s \subset V^{L_N},\, \zeta \subset Z^{L_N}}{\text{Minimum}} \frac{1}{2} \sum_{\omega_n \subset \Omega} \sum_{l_m \subset L_M} F_{nm}(v_s, \zeta)^2 \qquad (2)$$

in which,

v_s	Vector containing shear wave velocities associated with the L_N layers of a soil column,
V^{Ln}	Bounds for v_s defined as: $v_{sBE}/(1+COV) < v_s < v_{sBE}(1+COV)$, v_{sBE} is the best estimate from laboratory tests (median values) and COV represents variability of the tests (COV = 0.5 is used in this study),
ζ	Vector containing hysteretic damping values associated with the L_N layers of a soil column,
Z^{Ln}	Bounds for ζ and for low strain properties ζ is set at ζ_i = 1.5% constant,
ω_n	Circular frequency,
Ω	The analysis frequency range,
L_M	Set of Fourier spectral ratios being considered.

The target function in Equation (2) is defined as:

$$F_{nm}(v_s, \zeta) = R_{l_m}(\omega_n) - H_{l_m}(\omega_n, v_s, \zeta) \qquad (3)$$

in which,

$R_{lm}(\omega_n)$	Fourier ratios computed from the accelerometer recordings between the rock and the location l_m,
$H_{lm}(\omega_n, v_s, \zeta)$	Theoretical transfer function between the rock and the location l_m.

The theoretical transfer function is computed using the one-dimensional wave propagation theory. The conditional non-linear least square minimization problem, as defined in Equation (2), was solved using the modified Levenberg-Marquardt algorithm, which has been discussed extensively in the literature [11].

The Fourier ratio technique, as discussed above, has been implemented into the CARES program [12] in which $x = (v_s)$ and $\zeta = \zeta_i$ (set at 1.5% constant), and was used for identification of the low strain properties of both the old and new

free field points. As will be discussed later in this report, the strain-dependent modulus degradation relationships will be determined by fitting the free field records to several available laboratory tests by performing equivalent-linear convolution analysis.

ANALYSIS RESULTS AND DISCUSSIONS

The BNL free field analysis was performed using the techniques described above and the analysis results are discussed in this section. NUPEC provided recorded data for five earthquake events, including one major event with a maximum free field acceleration of 174 Gal. Table 1 summarizes these events with respect to their occurrence time, source location, magnitude, epicenter and focal distances from the site, as well as maximum acceleration induced in the free field.

Table 1. Earthquake Events Selected for Collaboration

Earthq No.	Earthquake Occurrence Time	Source Location East Longitude	Source Location North Latitude	Earthquake magnitude (M)	Epicenter /Focal distance (km)	Max old free field point acceleration GL-1.5m (Gal) NS	Max old free field point acceleration GL-1.5m (Gal) EW	Max new free field point acceleration GL-3.0m (Gal) NS	Max new free field point acceleration GL-3.0m (Gal) EW
34	03-05-1991	141'41.0	41'16.0	4	28/46	15.8	9.6		
89	12-28-1994	143'43.3	40'27.1	7.5	213/213	123.0	174.0		
131	02-17-1996	141'23.0	40'47.0	4.6	43/45	15.9	17.3	15.1	13.3
139	02-20-1997	142'52.0	41'45.0	5.6	140/146	9.3	8.9	11.4	11.6
157	01-03-1998	142'04.0	41'28.0	5.1	66/89	28.5	26.7	20.8	30.2

These earthquakes were first examined for their propagating mechanism in the free field using the Arias intensity in order to select those that are consistent with the 1-D site characterization for the prediction of the soil properties. Figures 1 and 2 show the Arias intensity plots for Earthquakes Nos. 34 and 89, x-component at the old free field point. As shown in Figure 1, a consistent upward energy built-up from the rock seismometer (GL –34.3m) to near surface seismometer (GL –1.5m) is clearly demonstrated. For earthquake No. 89 (Figure 2), the Arias intensity plot did not establish a clear upward intensity built-up to support the rock to surface energy movement, which is inconsistent with an upward vertically propagating pattern. Therefore, Earthquake No.34 was selected for the site response analysis to determine the low strain soil properties for the old free field point and Earthquake No. 89 was not used for this purpose because of its inconsistency with the 1D site characterization. For the new free field point, three earthquake events were provided by NUPEC for the free field analysis, as designated by No. 131, No. 139 and No. 157. The analysis using the Arias intensity to determine the energy movement of these seismic events in the free field was performed. An upward energy movement in the free field was demonstrated for these earthquakes. For instance, Figures 3 and 4 provide the Arias intensity plots for Nos. 139 and 157, x-component. Although any of the earthquakes could have been used, No. 139 was chosen for the site response analysis to determine the low strain soil properties because it induced much smaller ground shaking than the others.

The BNL approach for determining low-strain soil properties utilizes the Fourier ratio technique with the modified Levenburg-Marquadt least square algorithm, as described in the previous section. The NUPEC laboratory estimated soil properties were used to calculate the initial estimate of the soil transfer function (rock to surface), with 1.5 percent constant damping assumed for the low-strain soils. The modified Levenburg-Marquadt least square minimization algorithm was then applied in conjunction with the convolution analyses performed with the CARES program to correlate the predicted soil transfer function with the target Fourier ratio of the surface to rock seismometer recordings for an earthquake event. The iteration continued until a satisfactory correlation was achieved, and the predicted soil properties were back calculated by the CARES program. For the old free field point, Earthquake No.34 was used as the target and the computed rock-to-surface amplification was compared to the Fourier ratio of the surface to rock seismometer recordings, as shown in Figure 5. As displayed in this figure, an excellent match was achieved between the BNL prediction and the recording at the major peak near the soil frequency about 6.0 Hz. Although the BNL calculation did not predict well at the second peak in the transfer function (primarily due to the fact that a clearly defined second peak does not exist in the target soil amplification), the BNL prediction is believed to be adequate for computing the soil properties, since the soil response is primarily controlled by the first major peak in the transfer function. The BNL estimated soil profile for the old free-field point was then used to compute the free-field response in terms of response spectra, using the GEI (Geotechnical Engineers, Inc.) degradation model and the CARES program for an equivalent linear convolution analysis. In addition, the computed response spectra were compared to the recorded spectra at GL –1.5m and GL –13m with very good agreement. These results are presented in Figures 6 and 7.

The same process was used to develop the low-strain soil profile for the new free-field point, using Earthquake No.139. Figure 8 shows the comparisons of the computed rock-to-surface amplification to the Fourier ratio of the surface to rock seismometer recordings. Again, a good match was obtained at the first resonance peak. Response spectra were also computed and compared to the recordings at GL –3.0m (similar results were obtained for GL –6.8m) as plotted in Figure 9, which show excellent agreement between computed and recorded responses. Finally, the BNL estimated soil profiles for both old and new free field points are plotted together with the corresponding NUPEC laboratory data, as shown in Figure 10.

Furthermore, three published laboratory data on the strain dependent modulus degradation relationships were examined for the BNL predicted soil profiles for both old and new free field points. Figure 11 presents a comparison of the response spectra computed for the location GL –3.0m at the new free field point, using the three published laboratory data and Earthquake No 157. In this comparison, responses calculated using both GEI and EPRI 93 degradation models appear very close to each other and both are comparable to the recorded responses, while the response generated with the Geomatrix model appears less comparable to the recorded responses in both frequency content and amplitudes.

CONLUSION

As part of a collaborative research effort, NRC/BNL and NUPEC of Japan have been investigating the various aspects of the dynamic structure-soil-structure interaction (SSSI) effects on the seismic response of nuclear power plant (NPP) structures, both experimentally and analytically. In this paper, the BNL free field analysis was described, which was based on the Fourier ratio technique with the modified Levenburg-Marquadt least square minimization algorithm for the correlation with the recorded free-field seismic motions. In addition, Arias intensity was employed to identify the energy transmission mechanisms for the earthquakes traveling across the site. The BNL predicted low strain soil profiles for both the old and new free-field points were compared to the laboratory test data and differences to different degrees were observed, especially for the near surface soil layers. Finally, several published degradation data were examined and compared with the computed free field response to recordings. It was concluded that both GEI and EPRI 93 degradation models produce the free-field responses comparable to the recorded free-field recordings, and therefore, are equally applicable to the site.

DISCLAIMER NOTICE

This work was performed under the auspices of the U.S. Nuclear Regulatory Commission, Washington, D.C. The findings and opinions expressed in this paper are those of the authors, and do not necessarily reflect the views of the U.S. Nuclear Regulatory Commission, Brookhaven National Laboratory or the Nuclear Power Engineering Corporation.

REFERENCES

1. Fukuoka, A , "Dynamic Soil-Structure Interaction of Embedded Structure", Trans. 13th SmiRT, vol. III, Port Alegre, 1995.
2. Suzuki, A. et al., "Evaluation of Seismic Input Motions and Responses of Buildings in Nuclear Power Plants", Proceeding of the OECD/NEA Workshop on the Engineering Characterization of Seismic Input, Brookhaven National Laboratory, Upton, New York, November 15-17, 1999, NEA/CSNI/R(2000)2/Volume 2, January 2001.
3. Chin, M. M., et al., "Site Response Analysis of Vertical Excitation", ASCE, Geotechnical Earthquake Engineering and Soil Dynamics III, vol. 1, 1998.
4. Kurita, T., "Dynamic Characteristics of Soil Deposits Identified from Seismic Records", Trans. 14th SmiRT, Lyon, France,1997.
5. Geotechnical Engineers Inc (GEI), "Evaluation of Dynamic Soil Properties for F-Area Sand Filter Structures," Report Prepared for E.I. Dupont de Nemours &Co., 1983.
6. Lee, R.C., "Investigation of Nonlinear Dynamic Soil Properties at the Savannah River Site", Westinghouse Savannal River Site Report, WSRC-TR-96-0062, Rev.0, March 1996.
7. Geomatrix Consultants Inc., "Ground Motion Following Selection of SRS Design Basis Earthquake and Associated Deterministic Approach", WSRC Report AA20210s, Prepared for Westinghouse Savannah River Site, March 1991.
8. EPRI, "Guidelines for Determining Design Ground Motions," EPRI TR-102293, November 1993.
9. Arias, A., "A Measure of Earthquake Intensity," Seismic Design for Nuclear Power Plants, edited by R. Hansen, The MIT Press, 1970.
10. Harp, E.L., et al., "Shaking Intensity Thresholds for Rock Fall and Slides: Evidence from 1987 Whitter Narrows and Superstition Hill Earthquake Strong-Motion Records," Bulletin of Seismological Society of America, vol. 85, Dec. 1994.
11. Fletcher R., "A modified Marquadt Subroutine for Nonlinear Least Square Records," Harwell Report, AERE-R, 6799 1971.
12. Xu, J., "Integrated Software System for Seismic Evaluations of Nuclear Power Plant Structures", The International Journal of Computers & Structures, Vol.46, No.4, pp.717-723, 1993.

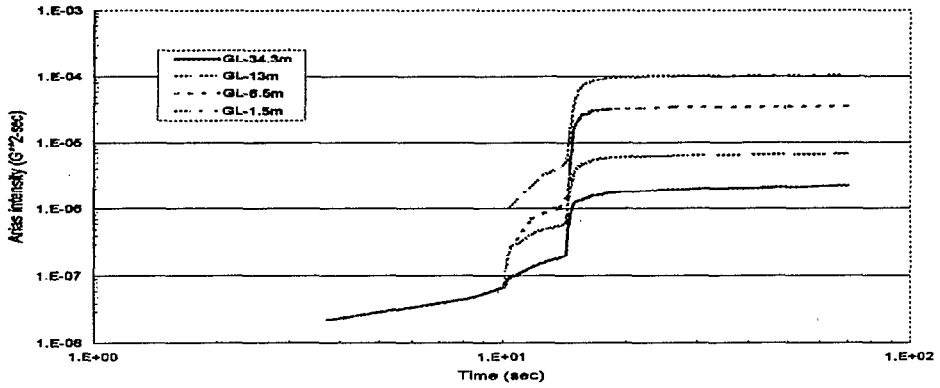

Figure 1. Arias intensities for the down-hole array for Earthquake 34x at Old Free Field Point.

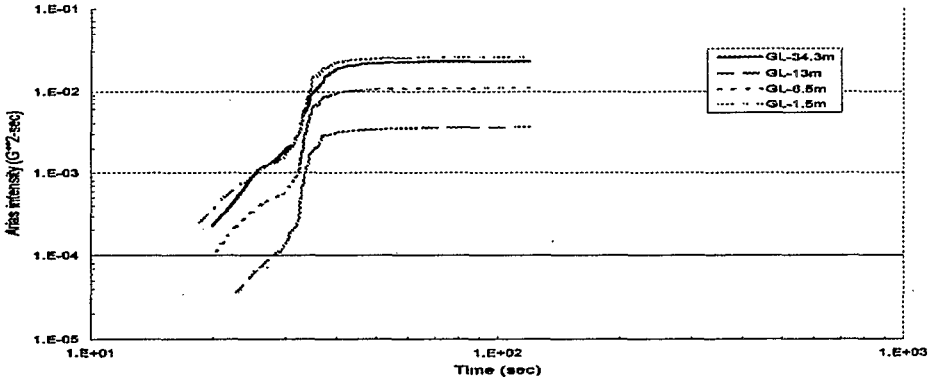

Figure 2. Arias intensities for the down-hole array for Earthquake 89x at Old Free Field Point.

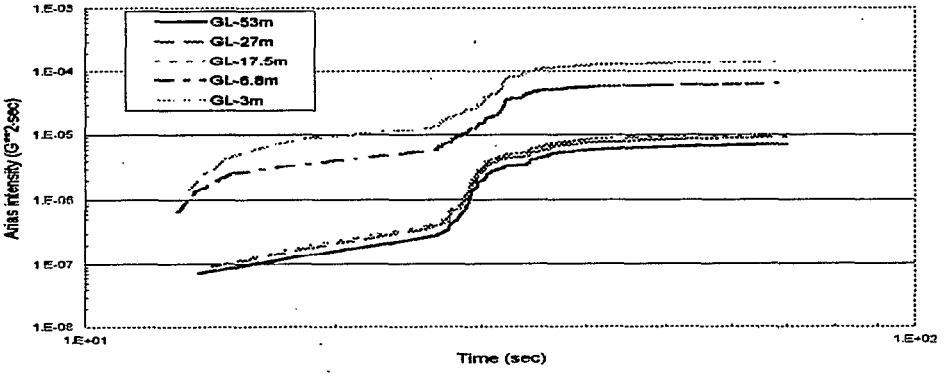

Figure 3. Arias intensities for the down-hole array for Earthquake 139x at New Free Field Point.

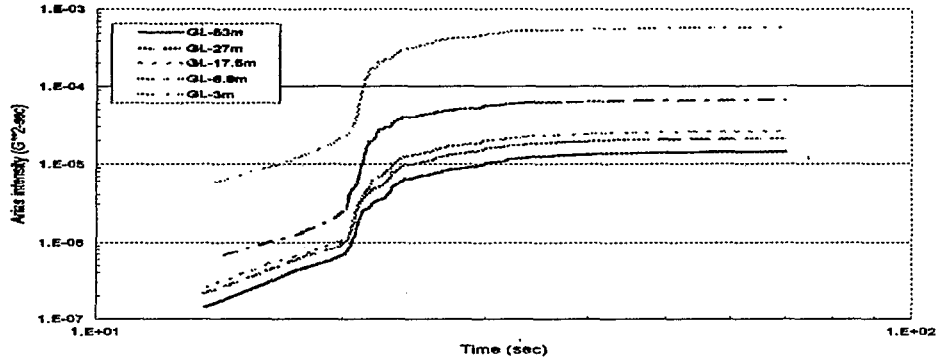

Figure 4. Arias intensities for the down-hole array for Earthquake 157x at New Free Field Point.

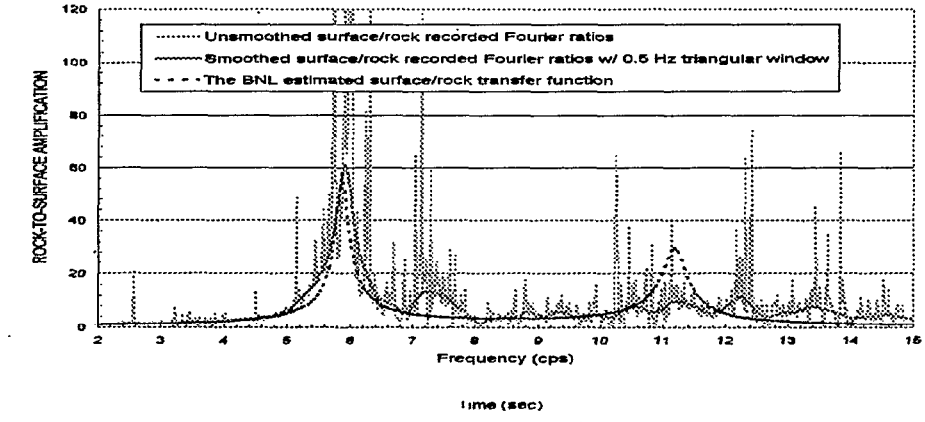

Figure 5. Predicted rock-to-surface amplification for Earthquake 34x at Old Free Field Point.

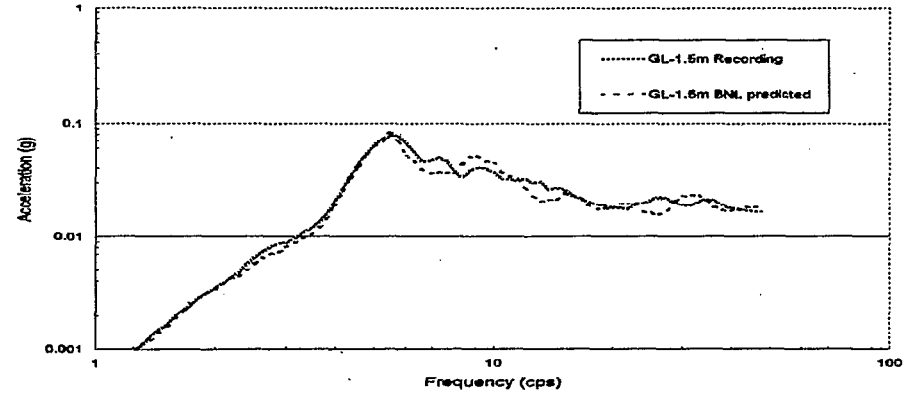

Figure 6. BNL predicted response spectrum at GL-1.5m, compared to the recording for Earthquake 34x at Old Free Field Point.

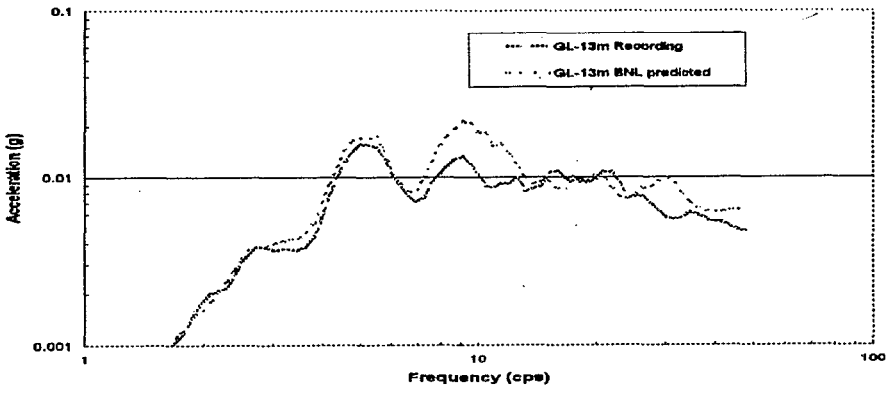

Figure 7. BNL predicted response spectrum at GL-13m, compared to the recording for Earthquake 34x at Old Free Field Point.

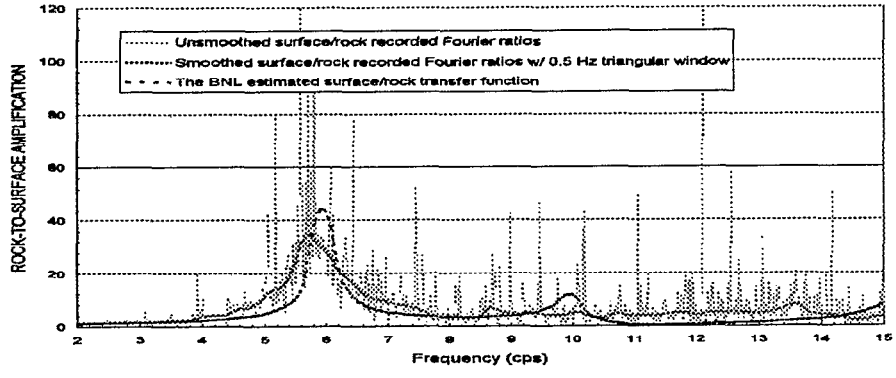

Figure 8. Predicted rock-to-surface amplification for Earthquake 139x at New Free Field Point

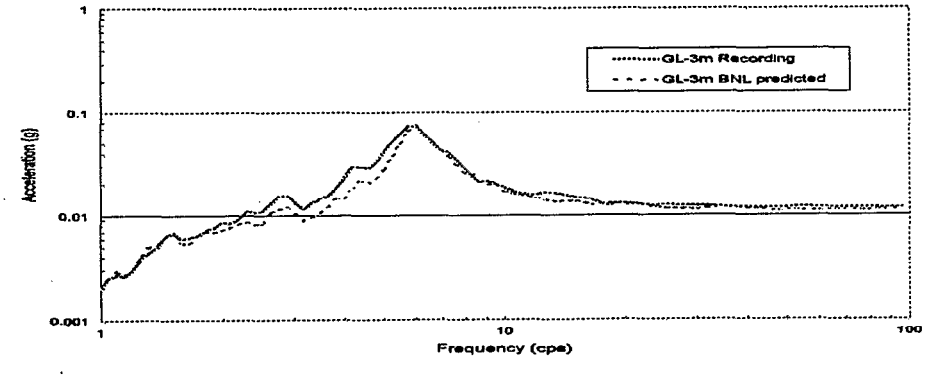

Figure 9. BNL predicted response spectrum at GL-3m, compared to the recording for Earthquake 139x at New Free Field Point.

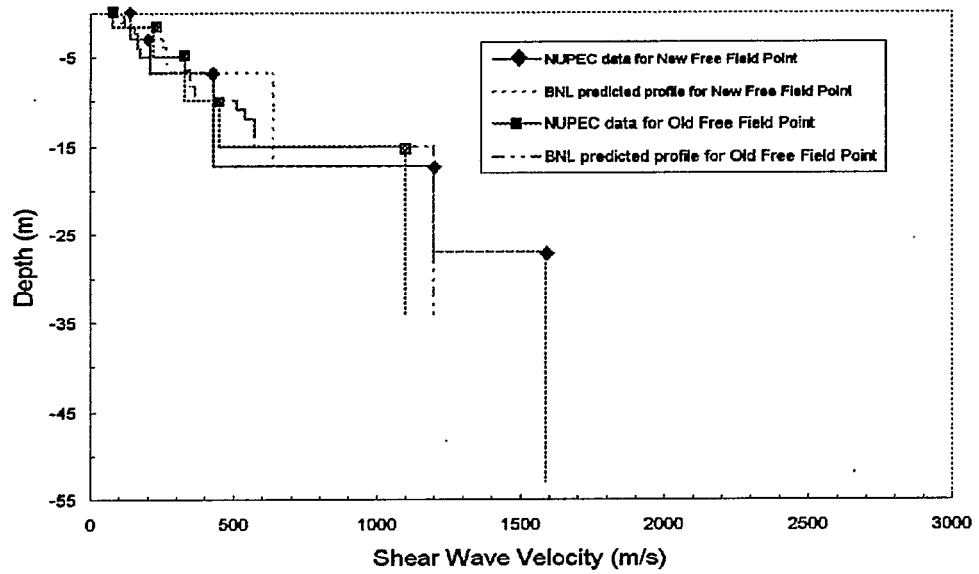

Figure 10. BNL predicted low strain soil profiles for New/Old Free Field Points.

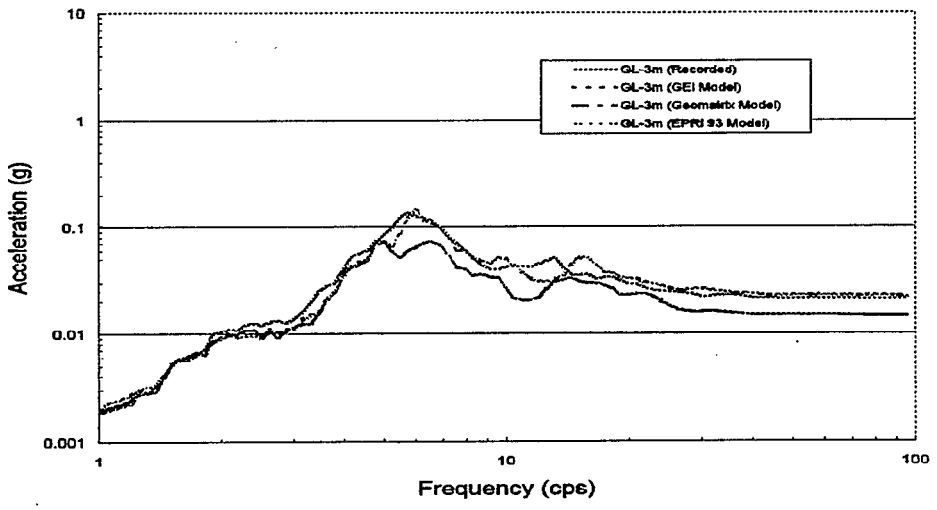

Figure 11. Comparison of response spectra using different degradation models for Earthquake 157x at New Free Field Point.